RESEARCH ARTICLE

Macromolecular Rapid Communications
www.mrc-journal.de

On-Chip Direct Laser Writing of PAN-Based Carbon Supercapacitor Electrodes

Andreas Hoffmann, Pablo Jiménez-Calvo, Joachim Bansmann, Volker Strauss, and Alexander J. C. Kuehne**

The carbonization of polyacrylonitrile (PAN) by direct laser writing to produce microsupercapacitors directly on-chip is reported. The process is demonstrated by producing interdigitated carbon finger electrodes directly on a printed circuit board (PCB), which is then employed to characterize the supercapacitor electrodes. By varying the laser power, the process can be tuned from carbonization to material ablation. This allows to not only convert pristine PAN films into carbon electrodes, but also to pattern and cut away non-carbonized material to produce completely freestanding carbon electrodes. While the carbon electrodes adhere well to the printed circuit board, non-carbonized PAN is peeled off the substrate. Specific capacities as high as 260 µF cm^{-2} are achieved in a supercapacitor with 16 fingers.

1. Introduction

Miniaturized electric double-layer capacitors—termed microsupercapacitors—enable integrated energy storage directly on the chip, facilitating self-sufficient devices without a large periphery for external power supply and management systems.[1–3] Such devices for on-chip energy storage could potentially transform the way we employ wearable and textile electronics and foster the development of autonomous microrobots.[4–6] Different classes of organic and inorganic materials have been explored for carbon-based microsupercapacitors electrodes, with the aim of increasing the surface area to yield acceptable capacitance despite their small size.[7–12] However, fabrication techniques to produce the required electrode geometries are limited to off-chip methods. The solvents or high processing temperatures employed to obtain carbonized, conductive electrode material are incompatible with typical electronic chip materials. Certainly, patterning and carbonization of carbon precursor materials remain possible off-chip; however, off-chip carbonization, in turn, requires precise and complicated placing, interfacing, and integration of the manufactured supercapacitor on the dedicated chip.[13]

We and others have previously reported on laser-induced carbonization of PAN-based carbon-fibers and other carbon-precursors.[14–18] Conventional carbonization of PAN is performed in convection ovens at temperatures >1000 °C.[19,20] By contrast, laser-induced carbonization is beneficial, as heat is locally produced in the focus of the laser, preventing exposure to high temperatures in undesired areas. Moreover, laser-carbonization is fast, potentially allowing pattern formation of carbonized PAN when scanning the laser focus across a film.[21]

However, pristine PAN is transparent in the visible and near IR spectrum, which requires the addition of a photosensitizer to enable its laser carbonization. CNTs are robust laser-absorbers and have previously been shown to improve the performance of carbonized materials by increasing their electrical conductivity[22] and surface area.[23]

Here, we demonstrate how interdigitated carbon electrodes can be directly laser-patterned into a film of CNT sensitized PAN to produce microsupercapacitors. We perform direct laser-writing on commercially available PCB to demonstrate that the laser-written carbon structures are well interfaced with the metallic current collectors on the PCB and that our laser process does not interfere with the materials of the substrate. The resulting supercapacitor electrodes are then characterized and benchmarked using an ionic liquid electrolyte.

2. Results and Discussion

PAN is a transparent polymer, which shows no absorption in the visible and near-infrared spectrum. To enable laser carbonization, an absorber is added, to facilitate absorption of the laser energy and transfer heat into the exposed PAN material. We have

A. Hoffmann, A. J. C. Kuehne
Institute of Organic and Macromolecular Chemistry
Ulm University
Albert-Einstein-Allee 11, 89081 Ulm, Germany
E-mail: alexander.kuehne@uni-ulm.de
P. Jiménez-Calvo, V. Strauss
Department of Colloid Chemistry
Max-Planck-Institute of Colloids and Interfaces
Am Mühlenberg 1, 14476 Potsdam, Germany
E-mail: volker.strauss@mpikg.mpg.de
J. Bansmann
Institute of Surface Chemistry and Catalysis
Ulm University
Albert-Einstein-Allee 47, 89069 Ulm, Germany

The ORCID identification number(s) for the author(s) of this article can be found under https://doi.org/10.1002/marc.202100731

DOI: 10.1002/marc.202100731

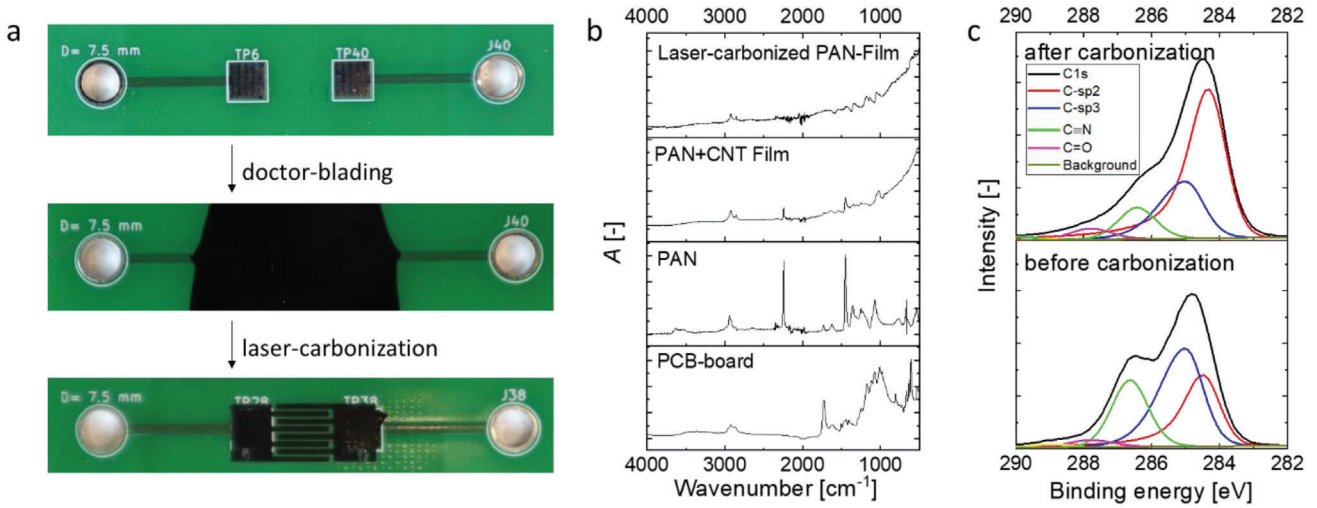

Figure 1. a) Photographs of the microcaps during progressing manufacturing stages. Bare PCBs containing the square silver electrodes, which act as current collectors. The current collectors connect the carbon electrodes to a read-out device via banana clips. The space between the collectors, as well as the current collectors themselves, are coated with a PAN-CNT composite film. In a second step, the film is laser-carbonized and patterned producing interdigitating electrodes. b) FT-IR-absorbance spectra of the bare PCB-board, PAN, the laser-absorbing PAN-CNT composite film, and laser-carbonized electrodes. c) XPS-spectra of PAN-CNT films before (bottom) and after (top) laser-carbonization.

previously employed graphene nanoplatelets as absorbers[14]; however, these fillers strongly increase the viscosity of the PAN solution, which is beneficial for fiber spinning but not necessarily beneficial for casting films. Therefore, we here make use of CNTs, which come as a dispersion in dimethyl sulfoxide. CNTs exhibit high conductivity, which is why we do not expect detrimental effects of the filler on the conductivity of the carbonized PAN material. We employ a concentration of 3 wt% of CNT per weight PAN, while the concentration of PAN in DMSO is 12 wt%. The concentration of 3 wt% CNT is optimized for sufficient absorption at the laser wavelength (CO_2, 10.6 µm) and maximum capacitance in the resulting carbon structures (see Figure S1, Supporting Information). We can spin-coat this PAN/CNT solution in DMSO onto almost any desired flat substrate and the resulting film thickness can be precisely tuned through the speed of rotation or the concentration of PAN in solution (see Figure S2, Supporting Information). However, to avoid coating the entire chip or PCB board with PAN/CNT in undesired areas, we here turn to pipette printing and subsequent doctor blading of the PAN/CNT solution. This way we are able to precisely deposit PAN/CNT onto the desired areas. As a substrate, we employ PCB with square silver collector electrodes of 16 mm^2 in area, which are separated by a distance of 7.5 mm. The collector electrodes are connected to a potentiostat via banana clips, which fit drillings in the PCB (see **Figure 1**).

We deposit the viscous PAN/CNT solution onto the PCB, by pipetting 2.5 mL of the viscous PAN/CNT solution as a grid of individual droplets. Closed films are drawn by doctor blading with a 30 µm gap into an ≈3 cm long stripe across the collector electrodes. The resulting films have a thickness of 20–21 µm after drying (see Figure S3, Supporting Information).

These films are irradiated with a CO_2 laser with a wavelength of 10.6 µm. In an attempt to replicate the thermal two-step treatment of stabilization and carbonization, we conduct laser exposure at an increasing power density in the air to generate laser-induced stabilization. However, we are not able to separate the exothermic stabilization event from carbonization. In contrast to carbonization, where increasing laser power density produces higher degrees of carbonization, for the stabilization step, there seems to exist a sharp threshold of 0.26 J mm^{-2}. Below this threshold, we do not see a change in the material properties or the infrared spectrum, in which stabilization is detectable by the disappearance of the corresponding nitrile band at 2442 cm^{-1} (see Figure 1b). Above the threshold we obtain conductive structures, indicating that we can conduct stabilization and carbonization in one step, despite the presence of air. Typically, thermal carbonization is conducted in the absence of air to avoid oxidation of the carbon material to CO_2. However, our laser carbonization is sufficiently fast, so that oxidation does not occur and the amount of sp^2-carbon increases to 52%, confirming successful laser carbonization (see Figure 1c). When we further increase the laser dose to 0.7 J mm^{-2} then we do no longer observe converted carbon structures, but instead, we observe the bare substrate, indicating the occurrence of an ablation process rather than pyrolytic carbonization (see **Figure 2**). This interval in power density is beneficial, as we can perform precise carbonization within this parameter window, while we can also employ the ablation process with power densities beyond this interval for precise removal of the PAN-precursor films. The underlying PCB board is not harmed by either process, as no visible or measurable material changes in infrared spectroscopy or conductivity occur.

We carry on to pattern interdigitated electrodes with eight or 16 fingers at 0.63 J mm^{-2}, which is the ideal dose for carbonization. In a second patterning step, we increase the power density to ablation and follow a trace between the electrode fingers to remove any non-carbonized material between the carbonized electrode fingers (see **Figure 3**).

Now that the carbonized electrode pattern is separated from the pristine area, the excessive non-carbonized PAN film can simply be peeled off the PCB (see Figure 3a). By contrast, the carbonized interdigitating supercapacitor electrodes adhere to the PCB (see Figure 3a: Video S1, Supporting Information). This

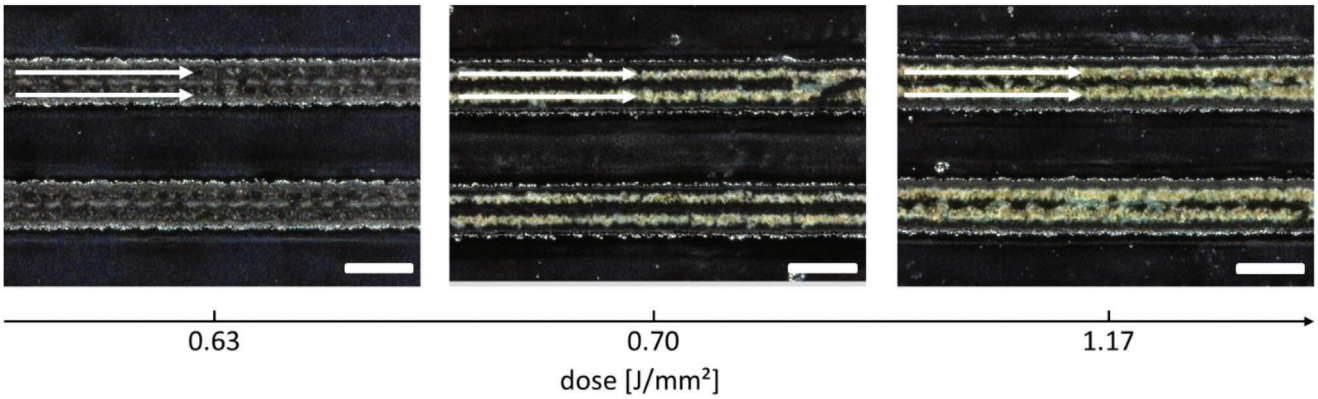

Figure 2. Variation of the laser dose for carbonization or ablation of PAN-films. White arrows indicate the pathway of the laser beam. A laser dose of 0.63 J mm^{-2} leads to carbonized structures, whereas increasing the dose to 0.70 J mm^{-2} leads to ablation of PAN material revealing the yellow/golden color of the PCB board. Doses higher than 1.17 J mm^{-2} lead to large area ablation, which limits the quality of the remaining PAN and carbon patterns. The scale bars represent 200 µm.

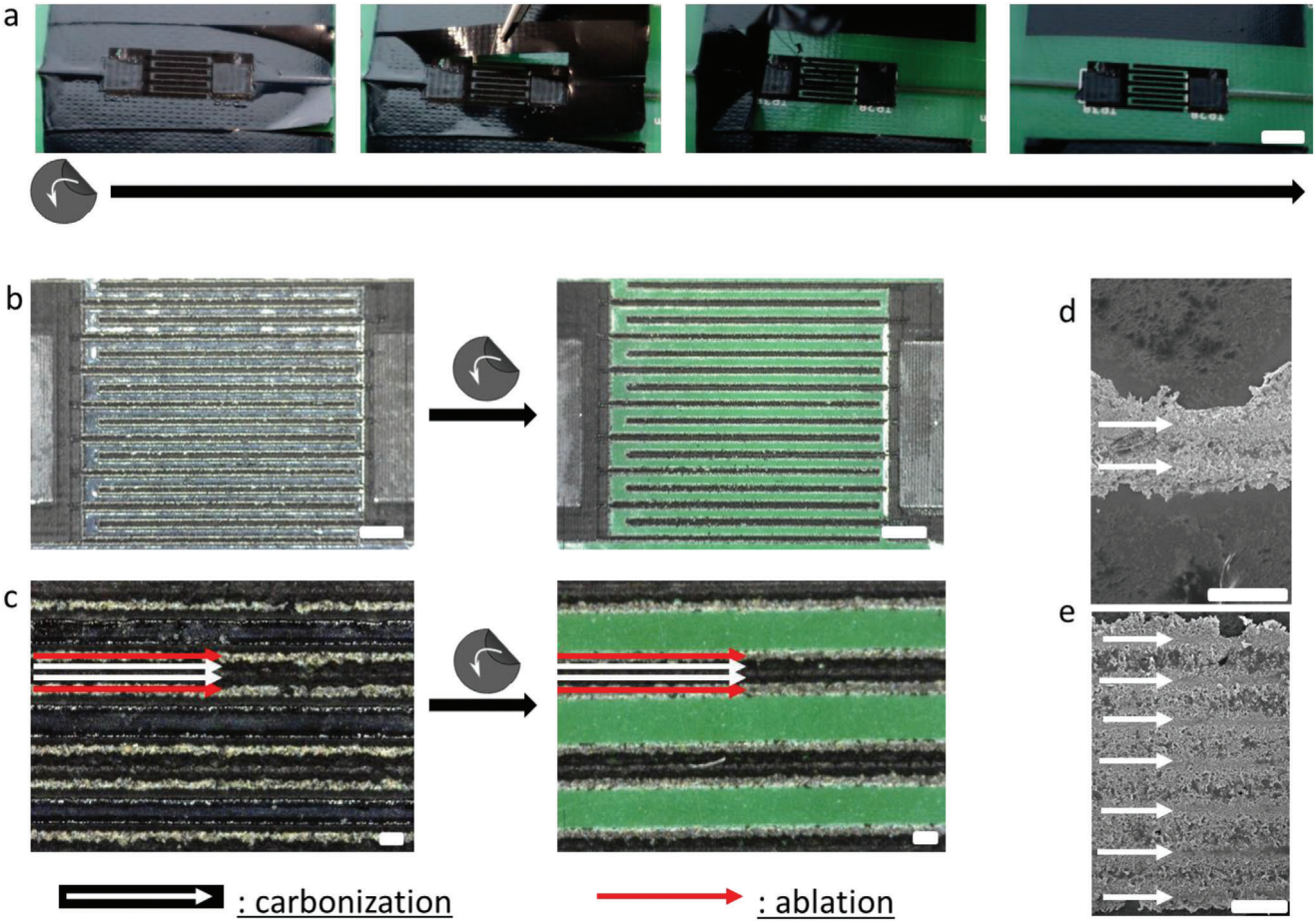

Figure 3. Laser carbonization and ablation to separate carbonized pattern from the non-carbonized film: a) The non-carbonized film is removed by peeling off with a pair of tweezers. The carbonized interdigitated electrode structure remains attached to the PCB. The scale bar represents 5 mm. b) Micrographs of the laser carbonized and ablated films before and after removal of the non-carbonized material. The scale bar represents 1 mm. c) Close-up on four electrodes and arrows indicating the laser paths for carbonization (white arrow) and ablation (red arrow) before and after removal of the non-carbonized PAN film. Scale bars indicate 100 µm. d) SEM-images of electrodes of 16-finger microcaps and e) 8-finger microcaps. The white arrows indicate the laser pathways for carbonization, producing electrodes of different widths. The scale bar indicates 100 µm.

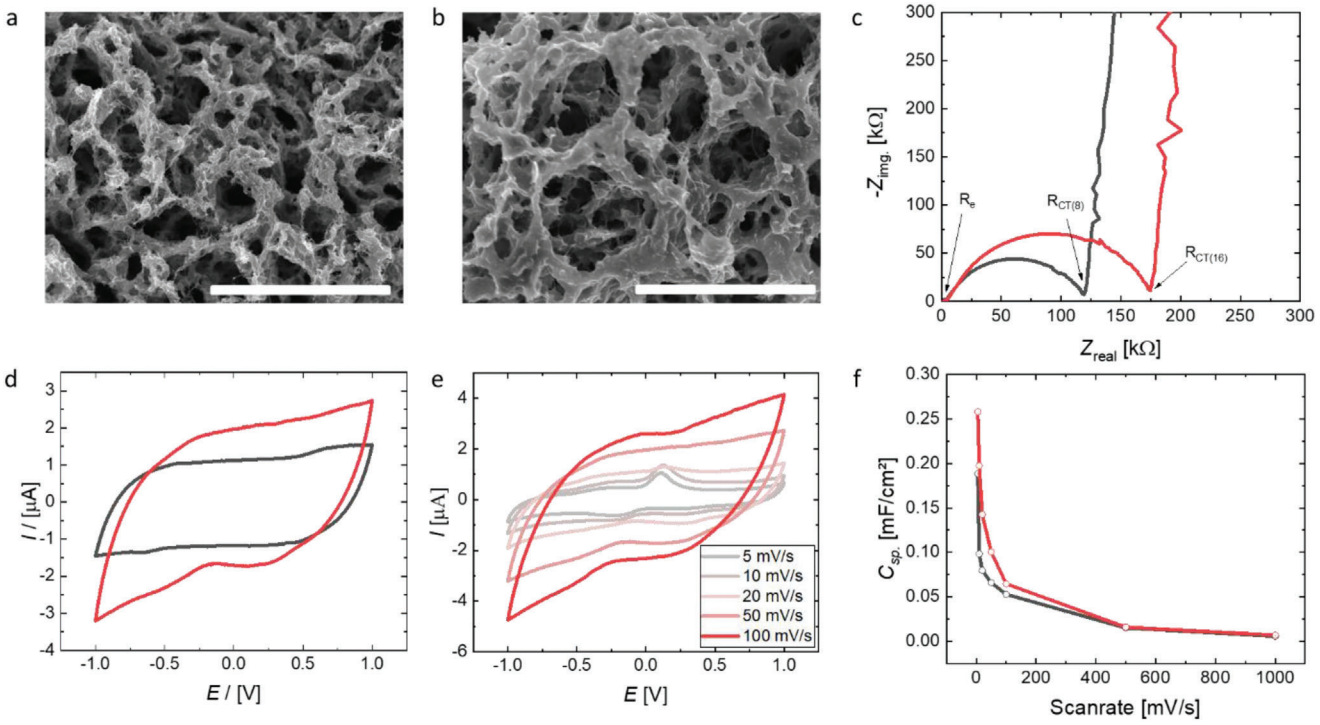

Figure 4. a) SEM-images of laser carbonized electrodes of the 8-finger and b) 16-finger pattern. The scale bars indicate 5 µm. c) Nyquist plots of laser-carbonized microcaps with 8- (black) and 16-finger (red) patterns. d) Cyclic voltammograms of 8- (black) and 16- finger (red) microcaps, recorded at 50 mV s^{-1}. e) Cyclic voltammograms of 16-finger microcaps, recorded at various scan rates. f) Specific capacitance of 8- (black) and 16-finger (red) microcaps at scan rates from 5 to 1000 mV s^{-1}.

way, the entire electrode structures including the sides of the electrode fingers down to the PCB substrate become accessible for the electrolyte in the final supercapacitor device. For 16 finger electrodes, the individual fingers are produced by scanning twice with the laser beam, followed by two additional scans for ablation and separation of the carbonized electrodes from the pristine PAN film (see Figure 3b–d). The eight finger devices are produced by seven laser traces next to each other (see Figure 3e). For eight fingers, the electrode width is $w = 510$ µm with a height of $h = 9.4$ µm at a spacing of $d = 290$ µm between electrodes; and for 16 fingers the dimensions are $w = 145$ µm, $h = 10.9$ µm, and $d = 263$ µm (see Figure S3, Supporting Information). The laser carbonization process produces electrodes of hierarchical porosity (see **Figure 4**a,b). This is a well-known feature of the fast laser carbonization process, where the gasses produced during carbonization are formed instantaneously, leading to the porous foam-like structure, with high surface area, which is beneficial for the capacitor performance.[14] Additionally, the compounded CNTs should contribute to the electrode performance. Analysis by scanning electron microscopy (SEM) shows that the remaining CNTs are intact after laser treatment and seem to percolate within the porous carbon structure, which could contribute to the electrical conductivity of the laser-carbonized material (Figure S4, Supporting Information).

Next, we test the performance of electrodes in electrochemical measurements. As electrolyte, we employ 20 µL of the ionic liquid 1-ethyl-3-methylimidazolium bis(trifluoromethylsulfonyl)imide (EMIM TFSI), which we deposit on the interdigitated finger electrodes in an inert nitrogen atmosphere. After an equilibration period of 12 h, we conduct electrochemical impedance spectroscopy and cyclovoltammetry. Nyquist plots of our eight or 16 finger electrodes show a semicircle at high frequencies and a steep increase with 85° phase angle at lower frequencies, indicating capacitive behavior (see Figure 4c). The semicircles intercept the *x*-axis at 2.3 kΩ for the eight finger electrodes and at 2.8 kΩ for the 16 finger electrodes. We interpret these values as the electrode resistance R_e (see Figure 4c).[24] By contrast, the charge transfer resistance R_{CT} is increased for the 16-finger microsupercapacitor (170 kΩ) compared to the eight-finger device (116 kΩ), which we account to the increased surface area in the 16-finger device (see Figure 4c). For the same reason, cyclovoltammetry shows that the double layer capacitance C_{sp} of the 16-finger device is much higher than in the 8-fingered device (see Figure 4d).

When we plot the specific area capacitance C_{sp} against the scan rate, we observe a similar trend for the 8 and 16-fingered electrode devices. However, the microsupercapacitor with 16-fingers achieves significantly higher $C_{sp} = 260$ µF cm^{-2} at low scan rates compared to $C_{sp} = 190$ µF cm^{-2} in the 8-finger device (see Figure 4d–f). This difference in performance indicates that there might be a greater number of accessible pores in the 16-finger device, which improves the capacitance compared to the 8-fingered microsupercapacitors with less overall interface. The achieved capacitances are of the same order of magnitude as for recently reported graphene-based finger capacitors of similar dimensions.[7] The microsupercapacitors retain their capacitance for 2000 cycles, which is comparable to other carbon electrodes (see Figure S5, Supporting Information).[25] Prolonged exposure of the electrodes to the ionic liquid electrolyte over the course of

7 days, does not lead to their delamination or changes in their electrochemical performance.

3. Conclusion

We have demonstrated how to achieve direct on-chip laser-carbonization of PAN films. Our specifically designed process has been used to fabricate carbon supercapacitor electrodes. We can precisely tune the process from carbonization to ablation, allowing us to remove any non-carbonized material to obtain free-standing interdigitating electrodes.

The developed process gives access to highly integrated energy storage devices of on-chip applications, which in the future might become even further miniaturized. Tuning of the exact porosity and potential post carbonization treatment to further activate the materials to increase the porosity might lead to even larger capacitances and better performance.

4. Experimental Section

Materials: Acrylonitrile homopolymer (M_w = 150 000 g mol^{-1}) was obtained from Dralon GmbH, Dimethylsulfoxide (DMSO) was obtained from Fisher Scientific, Acetone was obtained from Sigma–Aldrich, a CNT dispersion in DMSO with a weight content of 2 wt.% CNTs was obtained from Future Carbon GmbH, and 1-Ethyl-3-methylimidazolium bis(trifluoromethylsulfonyl)imide (EMIM TFSI; 99.5%) was obtained from Iolitec GmbH.

PAN-Deposition: The PCB board was designed with KiCad-software and manufactured by Aisler B.V. (Germany). PAN-CNT composite films were deposited on the PCB from a 12 wt.% homo-PAN solution in a mixture of DMSO:Acetone (V_{DMSO}:$V_{Acetone}$ = 4:1), containing 3 wt.% CNTs (related to the mass of PAN). PAN-CNT dispersion (2.5 mL) was deposited in a grid of droplets (microdrop technologies GmbH, Germany) between the collector electrodes over a length of 3 cm. A film was produced on the PCB, by moving a doctor blade (with a distance of 30 µm between the blade and the substrate) through the reservoir. The resulting film had a length of 3–6 cm and a width of 1–2 cm, covering the current collector and the space in between them. The coated PCB dried for 10 min at 110 °C prior to laser-carbonization.

Carbonization: Laser-carbonization was conducted with a high-precision laser engraver setup (Speedy 100, Trotec) equipped with a 60 W CO_2 laser. The laser beam was focused with a 2.5 in. lens providing a focal depth of ≈3 mm and a focus diameter of 170 µm. The center wavelength of the laser was 10.6 ± 0.03 µm. The laser was operated in a pulsed vector mode at 1000 Hz. Therefore, the resulting energy input onto the film (dose) was given per area in J mm^{-2}. The areal energy density results from the effective linewidth d (170 µm) of the carbonized structures obtained in the laser focus. The scanning speed υ', generically given in %, was converted into s m^{-1}. The effective output power P of the laser was measured with a Solo 2 (Gentec Electro-Optics) power meter. The line separation for the patterning of the interdigitated electrodes was 75 µm.

$$F = P \times \upsilon' \times d^{-1} \quad (1)$$

The unexposed, non-carbonized PAN-film was removed by peeling off.

Electrochemical Measurements: The produced microsupercapacitors were connected to an IviumStat.h potentiostat (Ivium technologies) via banana clips. All measurements were performed in a glove box, with a two-electrode setup and 20 µL of EMIM TFSI as an electrolyte. The electrolyte covered the whole electrode structure. The cyclic voltammograms were recorded at scan rates from 5 to 1000 mV s^{-1}. The specific capacitance was calculated by $C_{sp} = \frac{\int_{-1V}^{1V} I\,dU}{2 \cdot \nu \cdot 2U \cdot A}$, with the scan rate ν and the electrode area A. Impedance spectra were recorded from 5 MHz to 0.01 Hz at a voltage U of 0.1 V. The capacitance fatigue was determined by cycling 2000 voltammograms and displaying the capacity of every 100th cycle in Figure S5 (Supporting Information).

Instruments: IR-spectra were recorded on a PerkinElmer Spectrum two. SEM images were recorded on a Hitachi S-5200.

XPS was performed on a PHI 5800 ESCA system (Physical Electronics), using monochromatized Al Kα radiation (1486 eV). The pass energy for survey spectra was 93.9 eV, for detail spectra, 29.35 eV was used. The binding energies (BEs) of all spectra were calibrated with respect to the C (1s) peak. The data evaluation and peak convolution were performed using the commercial software CasaXPS 2.3.23PR1.0 (www.casaxps.com). A Tougaard-type background was subtracted before the peak-fitting process.

Supporting Information

Supporting Information is available from the Wiley Online Library or from the author.

Acknowledgements

The authors thank Carsten Johnigk and Dr. Christian Vedder both at ILT – Fraunhofer Institute for Laser Technology, Aachen, Germany for measuring the laser absorbance of PAN-CNT dispersions. The authors thank Dr. Christian Herbert and Dr. Andreas Wego both at Dralon GmbH for donating the PAN homopolymer. The authors thank Krisztian Herman for capacitance and conductivity measurements of CNT/C composites with various amounts of CNT. The authors thankfully acknowledge funding from the BMBF SuperCarbon (13XP5036E) and the Cluster of Excellence EXC2154 POLiS and the Max Planck Society for financial support.

Open Access funding enabled and organized by Projekt DEAL.

Conflict of Interest

The authors declare no conflict of interest.

Data Availability Statement

The data that support the findings of this study are available from the corresponding author upon reasonable request.

Keywords

carbonization, laser-induced carbonization, laser-pyrolysis, microcapacitors, polyacrylonitrile

Received: November 2, 2021
Revised: January 19, 2022
Published online: February 3, 2022

[1] P. Huang, C. Lethien, S. Pinaud, K. Brousse, R. Laloo, V. Turq, M. Respaud, A. Demortière, B. Daffos, P. L. Taberna, B. Chaudret, Y. Gogotsi, P. Simon, *Science* **2016**, *351*, 691.
[2] N. A. Kyeremateng, T. Brousse, D. Pech, *Nat. Nanotechnol.* **2017**, *12*, 7.
[3] F. Bu, W. Zhou, Y. Xu, Y. Du, C. Guan, W. Huang, *npj Flexible Electron.* **2020**, *4*, 31.
[4] R. Jia, G. Shen, F. Qu, D. Chen, *Energy Storage Mater.* **2020**, *27*, 169.
[5] Y. Lee, V. K. Bandari, Z. Li, M. Medina-Sánchez, M. F. Maitz, D. Karnaushenko, M. V. Tsurkan, D. D. Karnaushenko, O. G. Schmidt, *Nat. Commun.* **2021**, *12*, 4967.

[6] C. C. Mayorga-Martinez, J. G. S. Moo, B. Khezri, P. Song, A. C. Fisher, Z. Sofer, M. Pumera, *Adv. Funct. Mater.* **2016**, *26*, 6662.
[7] J. Ye, H. Tan, S. Wu, K. Ni, F. Pan, J. Liu, Z. Tao, Y. Qu, H. Ji, P. Simon, Y. Zhu, *Adv. Mater.* **2018**, *30*, 1801384.
[8] E. Hourdakis, A. G. Nassiopoulou, *PHYS STATUS SOLIDI A* **2020**, *217*, 1900950.
[9] J. Han, Y.-C. Lin, L. Chen, Y.-C. Tsai, Y. Ito, X. Guo, A. Hirata, T. Fujita, M. Esashi, T. Gessner, M. Chen, *Adv. Sci.* **2015**, *2*, 1500067.
[10] J.-H. Sung, S.-J. Kim, K.-H. Lee, *J. Power Sources* **2003**, *124*, 343.
[11] A. Eftekhari, L. Li, Y. Yang, *J. Power Sources* **2017**, *347*, 86.
[12] Y.-Z. Zhang, Y. Wang, T. Cheng, L.-Q. Yao, X. Li, W.-Y. Lai, W. Huang, *Chem. Soc. Rev.* **2019**, *48*, 3229.
[13] M. F. El-Kady, R. B. Kaner, *Nat. Commun.* **2013**, *4*, 1475.
[14] D. Go, P. Lott, J. Stollenwerk, H. Thomas, M. Möller, A. J. C. Kuehne, *ACS Appl. Mater. Interfaces* **2016**, *8*, 28412.
[15] D. Go, M. Opitz, P. Lott, K. Rahimi, J. Stollenwerk, H. Thomas, M. Möller, B. Roling, A. J. C. Kuehne, *J. Appl. Polym. Sci.* **2018**, *135*, 46398.
[16] S. Delacroix, H. Wang, T. Heil, V. Strauss, *Adv. Electron. Mater.* **2020**, *6*, 2000463.
[17] V. Strauss, M. Anderson, C. L. Turner, R. B. Kaner, *Mater. Today Energy* **2019**, *11*, 114.
[18] R. D. Rodriguez, S. Shchadenko, G. Murastov, A. Lipovka, M. Fatkullin, I. Petrov, T.-H. Tran, A. Khalelov, M. Saqib, N. E. Villa, V. Bogoslovskiy, Y. Wang, C.-G. Hu, A. Zinovyev, W. Sheng, J.-J. Chen, I. Amin, E. Sheremet, *Adv. Funct. Mater.* **2021**, *31*, 2008818.
[19] S. K. Nataraj, K. S. Yang, T. M. Aminabhavi, *Prog. Polym. Sci.* **2012**, *37*, 487.
[20] L. Zhang, A. Aboagye, A. Kelkar, C. Lai, H. Fong, *J. Mater. Sci.* **2014**, *49*, 463.
[21] H. Wang, S. Delacroix, O. Osswald, M. Anderson, T. Heil, E. Lepre, N. Lopez-Salas, R. B. Kaner, B. Smarsly, V. Strauss, *Carbon* **2021**, *176*, 500.
[22] T. Maitra, S. Sharma, A. Srivastava, Y. K. Cho, M. Madou, A. Sharma, *Carbon* **2012**, *50*, 1753.
[23] Y. Jeong, K. Lee, K. Kim, S. Kim, *Materials* **2016**, *9*, 995.
[24] B.-A. Mei, O. Munteshari, J. Lau, B. Dunn, L. Pilon, *J. Phys. Chem. C* **2018**, *122*, 194.
[25] C. Zequine, C. K. Ranaweera, Z. Wang, S. Singh, P. Tripathi, O. N. Srivastava, B. K. Gupta, K. Ramasamy, P. K. Kahol, P. R. Dvornic, R. K. Gupta, *Sci. Rep.* **2016**, *6*, 31704.

